HHS Public Access

Author manuscript

Spine J. Author manuscript; available in PMC 2016 May 16.

Published in final edited form as:

Spine J. 2013 March ; 13(3): 263–272. doi:10.1016/j.spinee.2012.12.004.

Injection of human umbilical tissue–derived cells into the nucleus pulposus alters the course of intervertebral disc degeneration in vivo

Steven K. Leckie, MD[a], **Gwendolyn A. Sowa, MD, PhD**[b], **Bernard P. Bechara, MSc**[b], **Robert A. Hartman, MSc**[a], **Joao Paulo Coelho, MSc**[b], **William T. Witt, MSc**[a], **Qing D. Dong, MSc**[a], **Brent W. Bowman, BA**[a], **Kevin M. Bell, MSc**[a], **Nam V. Vo, PhD**[a], **Brian C. Kramer, PhD**[c], and **James D. Kang, MD**[a]

[a]Department of Orthopedics, University of Pittsburgh Medical Center, 200 Lothrop St., Pittsburgh, PA 15213, USA

[b]Department of Physical Medicine & Rehabilitation, University of Pittsburgh Medical Center, 200 Lothrop St., Pittsburgh, PA 15213, USA

[c]Advanced Technology and Regenerative Medicine, Route 22 West, PO Box 151, Somerville, NJ 08876, USA

Abstract

Background context—Patients often present to spine clinic with evidence of intervertebral disc degeneration (IDD). If conservative management fails, a safe and effective injection directly into the disc might be preferable to the risks and morbidity of surgery.

Purpose—To determine whether injecting human umbilical tissue–derived cells (hUTC) into the nucleus pulposus (NP) might improve the course of IDD.

Design—Prospective, randomized, blinded placebo–controlled in vivo study.

Patient sample—Skeletally mature New Zealand white rabbits.

Outcome measures—Degree of IDD based on magnetic resonance imaging (MRI), biomechanics, and histology.

Methods—Thirty skeletally mature New Zealand white rabbits were used in a previously validated rabbit annulotomy model for IDD. Discs L2–L3, L3–L4, and L4–L5 were surgically exposed and punctured to induce degeneration and then 3 weeks later the same discs were injected with hUTC with or without a hydrogel carrier. Serial MRIs obtained at 0, 3, 6, and 12 weeks were analyzed for evidence of degeneration qualitatively and quantitatively via NP area and MRI Index. The rabbits were sacrificed at 12 weeks and discs L4–L5 were analyzed histologically. The L3–L4 discs were fixed to a robotic arm and subjected to uniaxial compression, and viscoelastic displacement curves were generated.

Results—Qualitatively, the MRIs demonstrated no evidence of degeneration in the control group over the course of 12 weeks. The punctured group yielded MRIs with the evidence of disc height loss and darkening, suggestive of degeneration. The three treatment groups (cells alone, carrier alone, or cells+carrier) generated MRIs with less qualitative evidence of degeneration than the

punctured group. MRI Index and area for the cell and the cell+carrier groups were significantly distinct from the punctured group at 12 weeks. The carrier group generated MRI data that fell between control and punctured values but failed to reach a statistically significant difference from the punctured values. There were no statistically significant MRI differences among the three treatment groups. The treated groups also demonstrated viscoelastic properties that were distinct from the control and punctured values, with the cell curve more similar to the punctured curve and the carrier curve and carrier+cells curve more similar to the control curve (although no creep differences achieved statistical significance). There was some histological evidence of improved cellularity and disc architecture in the treated discs compared with the punctured discs.

Conclusions—Treatment of degenerating rabbit intervertebral discs with hUTC in a hydrogel carrier solution might help restore the MRI, histological, and biomechanical properties toward those of nondegenerated controls. Treatment with cells in saline or a hydrogel carrier devoid of cells also might help restore some imaging, architectural, and physical properties to the degenerating disc. These data support the potential use of therapeutic cells in the treatment of disc degeneration.

Introduction

Intervertebral disc degeneration (IDD) is a frequently encountered condition by spine clinicians. In addition to adversely impacting quality of life, care for associated degenerative spinal pathology costs society over $40 billion annually in combined health-care spending and lost wages [1]. Patients who fail conservative management may become surgical candidates, although surgery does not reliably improve discogenic low back pain [2] and [3] and may induce adjacent segment degeneration [4]. The intervertebral disc (IVD) is a biologically harsh environment [5] and has a poor intrinsic healing capability [6]. Less invasive treatment paradigms that can safely and effectively alter the course of disc degeneration without hindering motion could have a significant impact on the lives of many patients.

Alternative biological treatments, such as growth factors, cell transplantation, and gene therapy [7] and [8], are under active investigation. Intervertebral disc degeneration is a complex process involving desiccation and loss of cellularity and extracellular matrix within the nucleus pulposus (NP) [9] and [10], and the rationale for cell-based therapy is to repopulate the disc so that the cells can renew synthesis of extracellular matrix and regenerate a biologically active environment. Cultured human amniocytes can be induced to differentiate into ectodermal and mesodermal cell types in vitro (including neuronal and osteogenic cells) even after several decades of cryopreservation [11]. In addition to cells found in the amniotic fluid, research has also focused on cells derived from Wharton's jelly [12], umbilical cord blood [13], and the placenta [14] and [15]. Human postpartum umbilical cord tissue is an attractive cell source because the cells are easily harvested from tissue that is abundantly available and otherwise discarded, as it is generated with every childbirth. Donor cords are easily collected without putting the donor at risk, and the cells do not carry the ethical conflicts that are associated with embryonic stem cells or fetal cells. Another advantage to human umbilical tissue–derived cells (hUTC) is that they can be manufactured from a single donor under Good Manufacturing Process regulations to create large cell banks

that may be used as needed. Human umbilical tissue–derived cells have recently been shown to secrete brain derived neurotrophic factor (a nerve growth factor) in vitro [16] and to reduce neurologic deficits in a rodent model of stroke after intravenous administration [17]. These studies demonstrate that transplanted hUTC are able to elicit a biological response.

Hydrogel NP replacement technology is also an active area of investigation. As the disc degenerates, the loss of disc height leads to an increased pressure on the facets and altered mechanical properties [18]. Hydrogels injected into the NP space can help restore the disc height (thereby normalizing biomechanical properties), and provide a scaffold for native cells to repopulate the disc and regenerate extracellular matrix [19] and [20].

In this study we investigate the utility of injecting hUTC directly into the NP in a surgical in vivo model of IDD. The hUTC were injected with and without a hydrogel carrier. This study is among the first to quantify the magnetic resonance imaging (MRI) and biomechanical responses to treatment in this degeneration model. We hypothesize that treating the degenerating IVD with either hUTC or a hydrogel carrier will slow the course of degeneration and that treating the disc with a combination of cells in a hydrogel carrier will have a more salutary effect than either intervention alone.

Methods

Rabbits

Thirty healthy skeletally mature New Zealand white rabbits were used in this study (female; age, 1 year; weight, 5 kg). They were split into nonpunctured control (n=6 rabbits, 18 discs), puncture (n=6 rabbits, 18 discs), puncture followed by injection of the carrier alone (n=6 rabbits, 18 discs), puncture followed by the injection of hUTC in phosphate-buffered saline (PBS) buffer (n=6 rabbits, 18 discs), and puncture followed by the injection of hUTC in a carrier (n=6 rabbits, 18 discs) (Table). The number of rabbits per group was selected based on our previous experience with this model and is typical for studies of this nature [7], [8], [21], [22], [23], [24], [25], [26] and [27]. This investigation was performed in full compliance with the Institutional Animal Care and Use Committee at our institution (protocols 0901919 and 0809294).

Sample preparation

Human umbilical cord tissue was obtained from a consented donor undergoing either vaginal or cesarean delivery. Human umbilical tissue–derived cells isolated and expanded from the umbilical cord of a single donor were supplied by Advanced Technologies and Regenerative Medicine, LLC. Briefly, the umbilical cord was manually minced and digested with a mixture of 0.5 U/mL collagenase (Nordmark, Uetersen, Germany), 5.0 U/mL dispase (Roche Diagnostics, Indianapolis, IN, USA), and 2 U/mL hyaluronidase (ISTA Pharmaceuticals, Irvine, CA, USA) until almost completely digested. The cell suspension was passed through a sieve to remove the undigested tissue, and the cells were centrifuged and seeded at 5,000 cells per cm2 on porcine gelatin–coated flasks in Growth Media 1 (Dulbecco's Modified Eagle Medium-low glucose [Cambrex/SAFC Biosciences, Lenexa, KS, USA], 15% [vol/vol] defined fetal bovine serum [FBS; HyClone, Logan, UT, USA],

0.001% betamercaptoethanol [Sigma, St Louis, MO, USA], and 50 U/mL penicillin and 50 μg/mL streptomycin [Lonza, Allendale, NJ, USA]). Cells were expanded in static T-flasks under standard tissue culture conditions in atmospheric oxygen with 5% carbon dioxide at 37° until reaching five population doublings (PD) and were banked. The cells were then expanded in static T-flasks to approximately 12 cumulative PD in Growth Media 2 (Dulbecco's Modified Eagle Medium-low glucose, 15% [vol/vol] defined fetal bovine serum [FBS; HyClone], and 100 U/mL penicillin and 100 μg/mL streptomycin [Invitrogen, Grand Island, NY, USA]) and were banked. Cells were then further expanded on Hillex II microcarriers (SoloHill Engineering, Ann Arbor, MI, USA) in spinner flasks (Corning, Corning, NY, USA) in Growth Media 2. The spinner flasks containing cells were placed on spinner plates set to 60 rpm, and the cells were cultured under standard conditions in atmospheric oxygen with 5% carbon dioxide at 37°C until they reached approximately 25 to 30 total cumulative PD. Cells were harvested from microcarriers using TrypLE (Invitrogen) and cryopreserved and stored at cryogenic temperatures. Aliquots of the cell bank were thawed for characterization testing that included viability, recovery, sterility, endotoxin, mycoplasma, karyology, and cell surface marker immunophenotyping to ensure safety and identity. Human umbilical tissue–derived cells have been found to be positive for CD10, CD13, CD44, CD73, CD90, and HLA-A, -B, and -C and negative for CD31, CD34, CD45, CD117, and HLA-DR, -DP, and -DQ [28]. All cell lots passed internal quality control according to these markers. Cells were tested at an early passage for viral pathogens by a polymerase chain reaction–based method to detect nucleic acid sequences specific to human immunodeficiency virus 1, human immunodeficiency virus 2, cytomegalovirus, hepatitis B virus, hepatitis C virus, human T-lymphotropic virus, and Epstein-Barr virus. Cells were stored at cryogenic temperatures until use and prepared for injection in the operating room before delivery. Immediately before the injection surgery, cell vials were thawed in a 37°C water bath and then washed with PBS. Aliquots of the cell suspension were removed and mixed with Trypan blue and counted with a hemocytometer. The cell concentration was adjusted to the appropriate density for delivery. The carrier solution was either PBS or an in situ hydrogel-forming carrier derived from the components of EVICEL (Omrix Biopharmaceuticals, Ltd, Somerville, NJ, USA). To load cells into the hydrogel, the cells were mixed with human fibrinogen (6.8–10.6 mg/mL) in PBS. This reagent was mixed with human thrombin (0.4–0.6 U/mL) in PBS. Gelation occurred shortly after mixing.

Puncture surgery

A previously validated animal model for IDD was used [21]. In a veterinary operating room, under sterile surgical conditions and general anesthesia, the rabbits' lumbar spines were exposed from a left anterolateral-retroperitoneal approach. The L4–L5 IVD was identified based on its position relative to the iliac crest and was punctured with a 16 G needle to a depth of 5 mm such that the tip of the needle was in the center of the disc. The needle entered the disc parallel to the end plates with the bevel pointed cephalad. Discs L3–L4 and L2–L3 were subsequently identified by direct visualization and palpation and punctured as mentioned previously. After surgery, the rabbits were housed in large private cages that allowed unrestricted movement. Annulotomy of a rabbit's IVD by this method induces a slow, reliable, reproducible cascade of degeneration, demonstrable by serial T2-weighted MRIs [22].

Injection surgery

The rabbits in the treatment groups returned to surgery 3 weeks after initial puncture surgery. The 3-week time-point was selected because in the original validation of the model [21], this was the earliest time at which degeneration could be detected on an MRI. The spine was exposed from a right anterolateral-retroperitoneal approach (contralateral to the previous puncture surgery). A Hamilton 100 μL syringe (1710TPLT; product #81041; Hamilton, Reno, NV, USA) and a Hamilton 30 G sharp-tipped needle with a plastic hub (KF 730 NDL 6/pack, 30G/2″; product # 90130) were used for therapeutic injections into the center of the NP. The small needle size was selected to avoid causing further degeneration to the disc [23]. For the carrier group, 15 μL of hydrogel was drawn up into the syringe and then slowly injected into each disc (in less than 4.5 minutes to facilitate liquid injection before gelation). For the cells+buffer (PBS) group, 105 hUTC in 15 μL of sterile PBS were injected into each disc. For the cells in the carrier group, 105hUTC in 15 μL of hydrogel carrier were injected. The injections were performed under c-arm guidance to confirm that the needle was in the center of the disc. All injections were performed at a deliberately slow and constant rate over the course of 1 minute to avoid rapid increases in the disc pressure and subsequent extrusion of materials. The rabbits were closed, revived, and cared for as described for the puncture surgery. Treated rabbits were returned to large private cages with unrestricted activity.

Magnetic resonance imaging

Sagittal MRIs were obtained at Time 0 (before annular puncture), 3 weeks (immediately before the injection surgery), 6 weeks, and 12 weeks (before sacrifice). A 3 Tesla Siemens magnet and a standard human knee coil were used to obtain T1- (repetition time=650 milliseconds, echo time=14 milliseconds, slice thickness=0.6 mm) and T2-weighted images (repetition time=3,800 milliseconds, echo time=114 milliseconds, slice thickness=0.6 mm). The rabbits were sedated and placed supine in a knee coil. The T1-weighted images were used to qualitatively check for any bone abnormalities in the spine. The T2-weighted images were used to quantify the amount of degeneration in the discs. The midsagittal slice of the T2-weighted sequences was identified by a blinded trained physician based on the width of the vertebral body, spinal cord, and spinous processes. A previously validated automated segmentation method was used [24] to identify the NP as the region of interest (ROI). In this segmentation method, a computer maps areas of similar MRI signal intensity on the midsagittal slice of each disc, and the largest concentric circle is selected as the ROI for the NP. This system eliminates human error and bias in selecting the MRI ROI. The MRI Index was calculated as the sum of the pixel area multiplied by the pixel intensity for each pixel within the ROI. The percentage NP area and MRI Index relative to control values at Week 0 were averaged across the three discs of interest and plotted against the time-points by a blinded investigator. Statistical analysis was performed with a two-way analysis of variance with an unequal number of observations. The categories were time-points and rabbit groups. If a statistical difference was found, the ad hoc analysis was a multiple comparison analysis based on Tukey's honestly significant difference criterion with a p value of .05.

Sacrifice and sample processing

All rabbits were sacrificed 12 weeks after the initial puncture surgery (after the final MRI was obtained). Immediately after euthanasia, the spines were dissected out en bloc. Disc L4–L5 was prepared for histological analysis. The discs were fixed and decalcified with Decalcifier I (Surgipath Medical Ind., Inc., Richmond, IL, USA) for 2 weeks and then dehydrated in a histology tissue processor and embedded in paraffin. Next, the discs were sectioned at a thickness of 5 μm in the sagittal plane. The sections were stained with hematoxylin and eosin (Fisher Scientific Co., Kalamazoo, MI, USA) using standard histology protocol, photographed using a Nikon E800 microscope (Nikon, Inc., Instrument Group, Melville, NY, USA), and analyzed by a blinded investigator.

Biomechanics

After sacrifice, disc L3–L4 was dissected out as a bone-disc-bone functional spinal unit for biomechanical analysis. Samples were cleaned of posterior elements, potted in epoxy resin, and mounted with custom fixtures in an axial testing machine controlled with a Matlab (Matlab R2008a; The Mathworks, Inc., Natick, MA, USA) fuzzy logic program. All discs were wrapped in saline-soaked gauze to minimize dehydration, and testing was performed on the same day as sacrifice. Specimens were preconditioned with 20 cycles of compressive loading (0–1.0 MPa, 0.1 mm/s) and then subjected to constant compression (1.0 MPa) for 1,100 seconds. This load target was selected because it is comparable with the pressures experienced by human IVDs during activities of daily living [29] (adjusted for the smaller size of the rabbit discs). The initial ramp phase was defined as the first 200 microseconds of testing, whereas the creep phase was defined as the remainder of testing. After testing, creep curves were fitted with a two-phase exponential model,

$$\frac{d(t)}{L_0}=\frac{1}{S_1}(1-e^{-S_1 t/\eta_1})+\frac{1}{S_2}(1-e^{-S_2 t/\eta_2})$$

where d(t) is the axial displacement over time, L0 is the applied axial load, S1 and S2 are elastic damping coefficients (N/mm), and η1 and η2 are viscous damping coefficients (Ns/mm). Average curves were generated and fitted with the exponential model for each condition, and the results were interpreted by a blinded investigator.

Randomization and blinding

Each rabbit had a four digit tattoo branded on one ear by the breeder. Rabbits were assigned to each treatment group in numerical order by ear tattoo. During the puncture surgery, the surgeon was blinded to which group each rabbit was assigned. Surgeon blinding was impossible during the treatment surgery because each treatment required special preparation on a back table immediately before the injection. While obtaining MRIs, the investigator was unaware of which rabbit belonged to which treatment group. Independent investigators analyzed the MRI, histology, and biomechanics data based on the numerical tattoo without knowing which group each rabbit belonged to.

Results

Rabbits

No deaths or adverse effects were observed in any groups as a result of the treatment. Some rabbits chewed at their surgical incisions, which were managed with local wound care and Elizabethan collars.

MRIs

The T1-weighted midsagittal MRIs of the L2–L3, L3–L4, and L4–L5 discs indicated no significant morphological changes or osteophyte formation (images not shown). The T2-weighted midsagittal MRIs of the discs in the control group demonstrated no evidence of degeneration. The punctured discs darkened and collapsed from 0 to 12 weeks as would be expected in a degeneration model. All three treatment groups demonstrated less qualitative evidence of disc degeneration than the punctured group, as shown in Fig. 1. The punctured (and not treated) discs showed the most degeneration, with a decrease of 59% in NP area and a decrease of 64% in MRI Index across time-points. All three treatment groups demonstrated less degeneration based on both total NP area and MRI Index than the punctured group. The carrier+cells group had the least decrease in area and MRI Index among the treated groups and most closely resembled the control group (Fig. 2). Statistical analysis with analysis of variance revealed MRI data for all the treatment and puncture groups at Weeks 6 and 12 was significantly different from Weeks 0 and 3. Moreover, MRI values from the puncture and all treatment groups at Weeks 6 and 12 were significantly different from the control group at those times. Although there was no significant difference among the treatment and the puncture groups at any time-point, there was a trend in which the puncture values were consistently lower than the treatment values. This result is true for both %area and %MRI Index data.

Biomechanics

Curves representing total load-normalized displacements (initial ramp phase and subsequent creep phase) are shown in Fig. 3. There are apparent differences among groups. Specifically, the curve generated by the control group is similar to the carrier+cells group, the punctured group is similar to the buffer+cells group, and the carrier group lies between these groups. Most of the variability between groups was from the initial ramp phase. Despite these trends, when the creep phase of the curve was fit with a two-phase exponential model, the early and late viscous and elastic damping coefficients did not yield any statistically significant differences (data not shown).

Histology

Representative sagittal cuts of the L4–L5 discs were stained with hematoxylin and eosin and inspected at ×20 and ×100 magnification (Fig. 4). Control discs maintained their architecture (Fig. 4A). As expected, the punctured discs demonstrated loss of NP cellularity and fibrosis, suggestive of degeneration (Fig. 4B). Punctured discs treated with the hydrogel carrier resulted in some loss of cellularity but maintained a robust extracellular matrix (Fig. 4C). Treatment with cells+buffer demonstrated relative preservation of the NP area, although

significant fibrosis was observed (Fig. 4D). Treatment with cells+carrier resulted in an improved cellularity and architecture compared with the punctured discs (Fig. 4E).

Discussion

This study uses a diverse range of outcome measures to demonstrate a response to a cellular therapy for disc degeneration. Based on MRI, histological, and biomechanical trends, injection into degenerating rabbit lumbar IVDs with hUTC in a hydrogel carrier might have a beneficial effect compared with either carrier alone or cells+buffer alone. However, the treatment groups were not significantly distinct. All three treatments trended toward an apparent benefit compared with the untreated punctured discs, although this also failed to achieve significance (Fig. 2). On MRI, the NP area and Index for all three treatment groups was between the control (nondegenerated) and punctured (most degenerated) conditions, indicating that treatment may have helped to partially delay disc height loss and signal intensity changes. However, the treatment failed to fully restore MRI parameters, as all groups were significantly distinct from the nondegenerated control group by 6 and 12 weeks. Axial loading generated displacement curves that appeared distinct for each condition. Previous biomechanical studies have detected differences between the punctured and nonpunctured discs [30] but few have looked at a treatment effect. In the annular puncture model, MRI evidence of disc degeneration correlates with disc hydration and proteoglycan content [25]. The viscous and elastic damping effects of uniaxial creep behavior are thought to be governed by the discs' proteoglycan content and collagen network [31], so it makes sense that biomechanical changes might correlate with MRI changes. Histology showed variable restorations of disc architecture and cellularity with treatment, which was consistent with the MRI findings. The clinical significance of any of these data is not entirely clear.

The cells+PBS group exhibited MRI data that fell between the control and punctured values and was very similar to the hydrogel carrier group's MRI data. However, this group's displacement curve was most similar to the punctured state, suggesting that although this treatment may have helped partially restore the NP area and signal intensity on MRI, it was not very effective at restoring the disc's native mechanical properties. Previous studies have used a punctured state in which saline was injected into the disc and X-ray and MRI evidence of degeneration still ensued [26]. This suggests that it was not the saline, but rather the cells that were responsible for the apparent response. It is possible that injecting cells in PBS had some efficacy in stalling the biochemical cascade of degeneration but that the injection eventually leaked out of the disc or was reabsorbed. This might explain why histology specimens from this group demonstrated sparse cellularity but a robust extracellular matrix (Fig. 4).

The carrier alone group generated MRI data that fell between the punctured and nonpunctured values. This is consistent with a previous study [27] in which a hydrogel was injected into the degenerating rabbit disc. In this study, as in our study, the rabbits' discs were punctured to induce degeneration and subsequently were evaluated by T2-weighted MRI and histology. The investigators found that after 1 week, both the implanted and punctured groups demonstrated MRI evidence of degeneration, but at 6 months the implanted discs showed MRI evidence of regeneration while the degenerating controls

continued to degenerate. In addition, histological examination revealed cell migration into the nucleotomy defect and tissue regeneration in the treated group. In our study, the displacement curve for the hydrogel group also fell between the punctured and nonpunctured states, suggesting that the hydrogel carrier might be capable of restoring some mechanical properties to the disc independent of any extracellular matrix synthesis by native or transplanted cells. Previous studies have also found that a hydrogel implanted into the NP space can exhibit creep under axial loading[32]. One might expect that the NP area on the MRI would have been better preserved by a space occupying therapeutic such as hydrogel or that there would be a more striking difference between the MRI generated measurements of NP area (essentially a mechanical property of the disc) and signal intensity (which is thought to reflect proteoglycan content [33]). The hydrogel may have interacted with the disc biology in a more complex manner or helped avert secondary degenerative changes that might occur as a result of the disc's initial collapse. Histology results from the carrier group demonstrate more cellularity than might be expected from a noncellular treatment, possibly indicating that the hydrogel provided a scaffold on which the native cells could repopulate the NP.

The cells+carrier group combined both the cell transplant and the hydrogel injection of the other two groups. This group had a consistent but a nonsignificant trend toward MRI degenerative measures that were better than the other two treatment groups (most similar to the control state, although still significantly distinct from control values). This group also had a displacement curve that was most similar to the control curve, suggesting a trend toward the best (albeit not statistically significant) mechanical response. The histological samples from this group demonstrated a notable increase in cellularity compared with the punctured group and a relative preservation of architecture but there is evidence of fibrosis. Although all of these measured outcomes indicate some improvement, they fail to demonstrate a full return to the nondegenerated state, and the differences among treatment groups are small.

There was no evidence of an immune response generated from transplanting human cells into a rabbit disc. None of the treated rabbits exhibited signs of illness, and there was no histological evidence of an inflammatory response. Given the paucity of vascularity within the disc, one would not expect an impressive immune response to any antigens delivered directly into this area. The effect of treatments that are misinjected into an immune privileged space, particularly into the dura, was not investigated in this study. An inflammatory response has been reported for stem cells that were injected into a spinal cord injury model in an effort to cure neurologic deficits [34]. The danger associated with material accidentally injected outside of the disc deserves further investigation.

Other cellular therapies under active investigation include chondrocyte allograft, NP cell allograft, and stem cell allograft. NP cells cocultured with bovine chondrocytes (which had been transduced with adenovirus carrying bone morphogenetic proteins 2, 4, 7, and 10) were stimulated to produce proteoglycan and collagen in vitro [35]. If applied to IDD, this technology could provide the disc with metabolically active chondrocytes and stimulate native NP cells to replenish the extracellular matrix. Although the precise mechanism by

which the hUTC influence the NP is unclear, it might be through a paracrine effect on the native NP cells, as was suspected for the bovine chondrocytes in this study by Zhang et al.

Transplanted human NP cells have been shown to survive in the NP for up to 24 weeks, and are capable of slowing the course of degeneration in vivo in the rabbit annulotomy model [36]. However, an important disadvantage of transplanting NP cells is that clinical access to healthy NP tissue is limited and in vitro expansion is difficult. Human umbilical tissue–derived cells, on the other hand, might be a more attractive cell source. Human postpartum umbilical tissue is readily available with each childbirth, and cells are easily harvested postpartum without the ethical conflicts that are associated with embryonic stem or fetal cells.

However, despite potential ethical concerns and difficulty of acquisition, the plasticity of stem cells makes them an intriguing transplant option. In vitro methods for inducing stem cells to differentiate into NP cells are under active investigation. Mesenchymal stem cells (MSCs) have been induced toward an NP cell phenotype by exposure to conditioned media from cultured NP cells [37], indicating that cytokines secreted by the NP are capable of steering stem cell differentiation. They have also been induced toward NP differentiation under hypoxic conditions (which are found at the center of the disc) [38]. Mesenchymal stem cells cocultured with NP cells in a three-dimensional matrix have been demonstrated to cause the cells to express a more chondrogenic gene expression profile [39]. This suggests that the mechanism by which the transplanted stem cells slow disc degeneration is via differentiation into NP cells followed by an increased production of the NP extracellular matrix. In addition, stem cells may help upregulate the viability of any surviving native NP cells in the degenerating disc [40]. Autologous MSCs transplanted into the degenerating disc have been shown to differentiate into cells expressing some of the major phenotypic characteristics of NP cells and to increase proteoglycan content in the rabbit annulotomy model [41], [42] and [43]. Similar biochemical results have been reported with transplantation of allograft bone [44] and adipose MSCs [45]. Human umbilical tissue–derived cells should not be confused with stem cells (as hUTC are terminally differentiated), but these studies in general support the potential for a cell-based therapy in a harsh biochemical environment [46]. It would be interesting to directly compare different cell types for efficacy at preventing disc degeneration. Bone marrow–derived MSCs were recently injected into the degenerating discs of human subjects, and the authors report improvement in both patient symptoms and MRI criteria [47] and [48]. Human umbilical tissue–derived cells require further in vitro and in vivo efficacy and safety testing before we would consider human trials.

The major limitation of this study is the lack of a biochemical analysis. It would have been informative to characterize the cell types of the NP on sacrifice to determine the fate of the transplanted cells. It remains unclear whether the cells are responsible for a sustained response, or whether they exert a transient response on injection and then expire. The precise mechanism by which the cells act on the disc also remains uncertain. Likewise, testing for whether the treated discs had generated new extracellular matrix (by assaying for proteoglycan and collagen content) would have been strong proof of efficacy. The sample size and time course, although small, are comparable with several previously published

studies that used similar methods [7], [8], [21], [22], [23], [24], [25],[26] and [27]. Although statistical significance was not achieved for some comparisons (such as between punctured and carrier MRI values), consistent trends were noted for each rabbit within a group. It is unclear for how long the transplanted cells might survive in the host environment, but demonstrating long term efficacy would be an important step in determining whether the treatment is worthwhile. Finally, rabbits are quadrupeds, and the annulotomy model and treatments may behave differently under bipedal conditions. However, there is biomechanical evidence to suggest that viscoelastic properties of rabbit discs under axial load might be translatable to human cadaver discs when normalized for disc size [49].

We have detected subtle histological, biomechanical, and imaging changes among differently treated groups in an in vivo rabbit model for disc degeneration, with only a modest sample size and short term follow-up. These results should be translated with caution to the human condition. Future translational work will be needed to elucidate whether these differences have any clinical significance. However, we have shown preliminary evidence that hUTC, if injected early in the degeneration cascade, might slow the course of degeneration. Transplanting hUTC in a hydrogel matrix into the degenerating IVD merits continued investigation.

References

1. Spine: low back and neck pain. Available at: www.boneandjointburden.org.
2. Fritzell P, Hagg O, Wessberg P. 2001 Volvo Award Winner in clinical studies: lumbar fusion versus nonsurgical treatment for chronic low back pain. Spine. 2001; 26:2521–2534. [PubMed: 11725230]
3. Bono C, Lee C. Critical analysis of trends in fusion for degenerative disc disease over the past 20 years: influence of technique on fusion rate and clinical outcome. Spine. 2004; 29:455–463. discussion Z455. [PubMed: 15094543]
4. Park P, Garton H, Gala V, et al. Adjacent segment disease after lumbar or lumbosacral fusion: review of the literature. Spine. 2004; 29:1938–1944. [PubMed: 15534420]
5. Holm S, Maroudas A, Urban J, et al. Nutrition of the intervertebral disc: solute transport and metabolism. Connect Tissue Res. 1981; 8:101–119. [PubMed: 6453689]
6. Bradford D, Cooper K, Oegema T. Chymopapain, chemonucleolysis, and nucleus pulposus regeneration. J Bone Joint Surg Am. 1983; 65:1220–1231. [PubMed: 6361035]
7. Nishida K, Kang J, Gilbertson L, et al. 1999 Volvo Award Winner in Basic Science studies: modulation of the biological activity of the rabbit intervertebral disc by gene therapy: an in vivo study of adenovirus-mediated transfer of the human transforming growth factor B1 encoding gene. Spine. 1999; 24:2419–2425. [PubMed: 10626303]
8. Leckie S, Bechara B, Hartman R, et al. 2011 NASS Outstanding Paper Award in Basic Science: injection of AAV2-BMP2 and AAV2-TIMP1 into the nucleus pulposus slows the course of intervertebral disc degeneration in an in vivo rabbit model. Spine J. 2012; 12:1–24. [PubMed: 22209241]
9. Pearce R, Grimmer B, Adams M. Degeneration and the chemical composition of the human intervertebral disc. J Orthop Res. 1987; 5:198–205. [PubMed: 3572589]
10. Urban J, McMullen J. Swelling pressure of the intervertebral disc: influence of proteoglycan and collagen contents. Biorheology. 1985; 22:145–157. [PubMed: 3986322]
11. Woodbury D, Kramer B, Reynolds K, et al. Long term cryopreserved amniocytes retain proliferative capacity and differentiate to ectodermal and mesodermal derivatives in vitro. Mol Reprod Dev. 2006; 73:1463–1472. [PubMed: 16894552]
12. Mitchell K, Weiss M, Mitchell B, et al. Matrix cells from Wharton's jelly form neurons and glia. Stem Cells. 2003; 21:50–60. [PubMed: 12529551]

13. Lee O, Ruo T, Chen W, et al. Isolation of multipotent mesenchymal stem cells from umbilical cord blood. Blood. 2004; 103:1669–1675. [PubMed: 14576065]
14. Fukuchi Y, Nakajima H, Sugiyama D, et al. Human placenta-derived cells have mesenchymal stem/progenitor cell potential. Stem Cells. 2004; 22:649–658. [PubMed: 15342929]
15. Anker P, Scherjon S, Kleijburg-van der Keur C, et al. Isolation of mesenchymal stem cells of fetal or maternal origin from human placenta. Stem Cells. 2004; 22:1338–1345. [PubMed: 15579651]
16. Alder J, Kramer B, Hoskin C, Thakker-Varia S. Brain-derived neurotrophic factor produced by human umbilical tissue-derived cells is required for its effect on hippocampal dendritic differentiation. Dev Neurobiol. 2012; 72:755–756. [PubMed: 21954108]
17. Zhang L, Li Y, Zhang C, et al. Delayed administration of human umbilical tissue-derived cells improved neurological functional recovery in a rodent model of focal ischemia. Stroke. 2011; 42:1437–1444. [PubMed: 21493915]
18. Leckie S, Kang J. Recent advances in nucleus pulposus replacement technology. Curr Orthop Pract. 2009; 20:222–226.
19. Leone G, Torricelli P, Chiumiento A, et al. Amidic alginate hydrogel for nucleus pulposus replacement. J Biomed Mater Res A. 2008; 84:391–401. [PubMed: 17618483]
20. Halloran D, Grad S, Stoddart M, et al. An injectable cross-linked scaffold for nucleus pulposus regeneration. Biomaterials. 2008; 29:438–447. [PubMed: 17959242]
21. Sobajima S, Kompel J, Joseph K, et al. A slowly progressive and reproducible animal model of intervertebral disc degeneration characterized by MRI, x-ray, and histology. Spine. 2005; 30:15–24. [PubMed: 15626975]
22. Masuda K, Aota Y, Muehlman C, et al. A novel rabbit model of mild, reproducible disc degeneration by anulus needle puncture: correlation between the degree of disc injury and radiological and histological appearances of disc degeneration. Spine. 2005; 30:5–14. [PubMed: 15626974]
23. Elliott D, Yerramalli C, Beckstein J, et al. The effect of relative needle diameter in puncture and sham injection animal models of degeneration. Spine. 2008; 33:588–596. [PubMed: 18344851]
24. Bechara B, Leckie S, Bowman B, et al. Application of a semi-automated contour segmentation tool to identify the intervertebral nucleus pulposus in MR images. Am J Neuroradiol. 2010; 31:1640–1644. [PubMed: 20581067]
25. Kim S, Yoon T, Li J, et al. Disc degeneration in the rabbit: a biochemical and radiological comparison between four disc injury models. Spine. 2004; 30:33–37. [PubMed: 15626978]
26. An H, Takegami K, Kamada H, et al. Intradiscal administration of osteogenic protein-1 increases intervertebral disc height and proteoglycan content in the nucleus pulposus in normal adolescent rabbits. Spine. 2005; 30:25–31. [PubMed: 15626976]
27. Abushi, Endres M, Cabraja M, et al. Regeneration of intervertebral disc tissue by resorbable cell-free polyglycolic acid-based implants in a rabbit model of disc degeneration. Spine. 2008; 33:1527–1532. [PubMed: 18520635]
28. Lund R, Wang S, Lu B, et al. Cells isolated from umbilical cord tissue rescue photoreceptors and visual functions in a rodent model of retinal disease. Stem Cells. 2007; 25:602–611. [PubMed: 17053209]
29. Wilke HJ, Neef P, Caimi M, et al. New in vivo measurements of pressures in the intervertebral disc in daily life. Spine. 1999; 24:755–762. [PubMed: 10222525]
30. Johannessen W, Cloyd J, O'Connell G, et al. Trans-endplate nucleotomy increases deformation and creep response in axial loading. Ann Biomed Eng. 2006; 34:687–696. [PubMed: 16482409]
31. Boxberger J, Sen S, Yerramalli C, Elliot D. Nucleus pulposus glycosaminoglycan content is correlated with axial mechanics in rat lumbar motion segments. J Orthop Res. 2006; 24:1906–1915. [PubMed: 16865712]
32. Freemont T, Saunders B. pH-responsive microgel dispersions for repairing damaged load-bearing soft tissue. Soft Matter. 2008; 4:919–924.
33. Benneker L, Heini P, Anderson S, et al. Correlation of radiographic and MRI parameters to morphological and biochemical assessment of intervertebral disc degeneration. Eur Spine J. 2005; 14:27–35. [PubMed: 15723249]

34. Samdani, Paul C, Betz R, et al. Transplantation of human marrow stromal cells and mono-nuclear bone marrow cells into the injured spinal cord. Spine. 2009; 34:2605–2612. [PubMed: 19881401]
35. Zhang Y, Li Z, Thonar E, et al. Transduced bovine articular chondrocytes affect the metabolism of cocultured nucleus pulposus cells in vitro: implications for chondrocyte transplantation into the intervertebral disc. Spine. 2005; 30:2601–2607. [PubMed: 16319745]
36. Iwashina T, Mochida J, Sakai D, et al. Feasibility of using a human nucleus pulposus cell line as a cell source in cell transplantation therapy for intervertebral disc degeneration. Spine. 2006; 31:1177–1186. [PubMed: 16688029]
37. Li H, Zou X, Baatrup A, et al. Cytokine profiles in conditioned media from cultured human intervertebral disc tissue: implications of their effect on bone marrow stem cell metabolism. Acta Orthop. 2005; 76:115–121. [PubMed: 15788319]
38. Risbud M, Albert T, Guttapalli A, et al. Differentiation of mesenchymal stem cells towards a nucleus pulposus-like phenotype in vitro: implications for cell-based transplantation therapy. Spine. 2004; 29:2627–2632. [PubMed: 15564911]
39. Vadala G, Studer R, Sowa G, et al. Coculture of bone marrow mesenchymal stem cells and nucleus pulposus cells modulates gene expression profile without cell fusion. Spine. 2008; 33:870–876. [PubMed: 18404106]
40. Yamamoto Y, Mochida J, Sakai D, et al. Upregulation of the viability of nucleus pulposus cells by bone marrow-derived stromal cells: significance of direct cell-to-cell contact in coculture system. Spine. 2004; 29:1508–1514. [PubMed: 15247571]
41. Sakai D, Mochida J, Iwashina T, et al. Differentiation of mesenchymal stem cells transplanted to a rabbit degenerative disc model: potential and limitations for stem cell therapy in disc degeneration. Spine. 2005; 30:2379–2387. [PubMed: 16261113]
42. Sakai D, Mochida J, Yamamoto Y, et al. Transplantation of mesenchymal stem cells embedded in atelocollagen gel to the intervertebral disc: a potential therapeutic model for disc regeneration. Biomaterials. 2003; 24:3531–3541. [PubMed: 12809782]
43. Sakai D, Mochida J, Iwashina T, et al. Regenerative effects of transplanting mesenchymal stem cells embedded in atelocollagen to the degenerated intervertebral disc. Biomaterials. 2006; 27:335–345. [PubMed: 16112726]
44. Zhang Y, Guo X, Xu X, et al. Bone mesenchymal stem cells transplanted into rabbit intervertebral discs can increase proteoglycans. Clin Orthop Relat Res. 2005; 430:219–226. [PubMed: 15662327]
45. Lu Z, Zandieh Doulabi B, Wuisman P, et al. Differentiation of adipose stem cells by nucleus pulposus cells: configuration effect. Biochem Biophys Res Commun. 2007; 359:991–996. [PubMed: 17572383]
46. Wuertz K, Godburn K, Neidlinger-Wilke C, et al. Behavior of mesenchymal stem cells in the chemical microenvironment of the intervertebral disc. Spine. 2008; 33:1843–1849. [PubMed: 18670337]
47. Orozco L, Soler R, Morera C, et al. Intervertebral disc repair by autologous mesenchymal bone marrow cells: a pilot study. Transplantation. 2011; 92:822–828. [PubMed: 21792091]
48. Yoshikawa T, Ueda Y, Miyazaki K, et al. Disc regeneration therapy using marrow mesenchymal cell transplantation: a report of two case studies. Spine. 2010; 35:E475–E480. [PubMed: 20421856]
49. Beckstein J, Sen S, Schaer T, et al. Comparison of animal discs used in disc research to human lumbar discs: axial compression mechanics and glycosaminoglycan content. Spine. 2008; 33:E166–E173. [PubMed: 18344845]

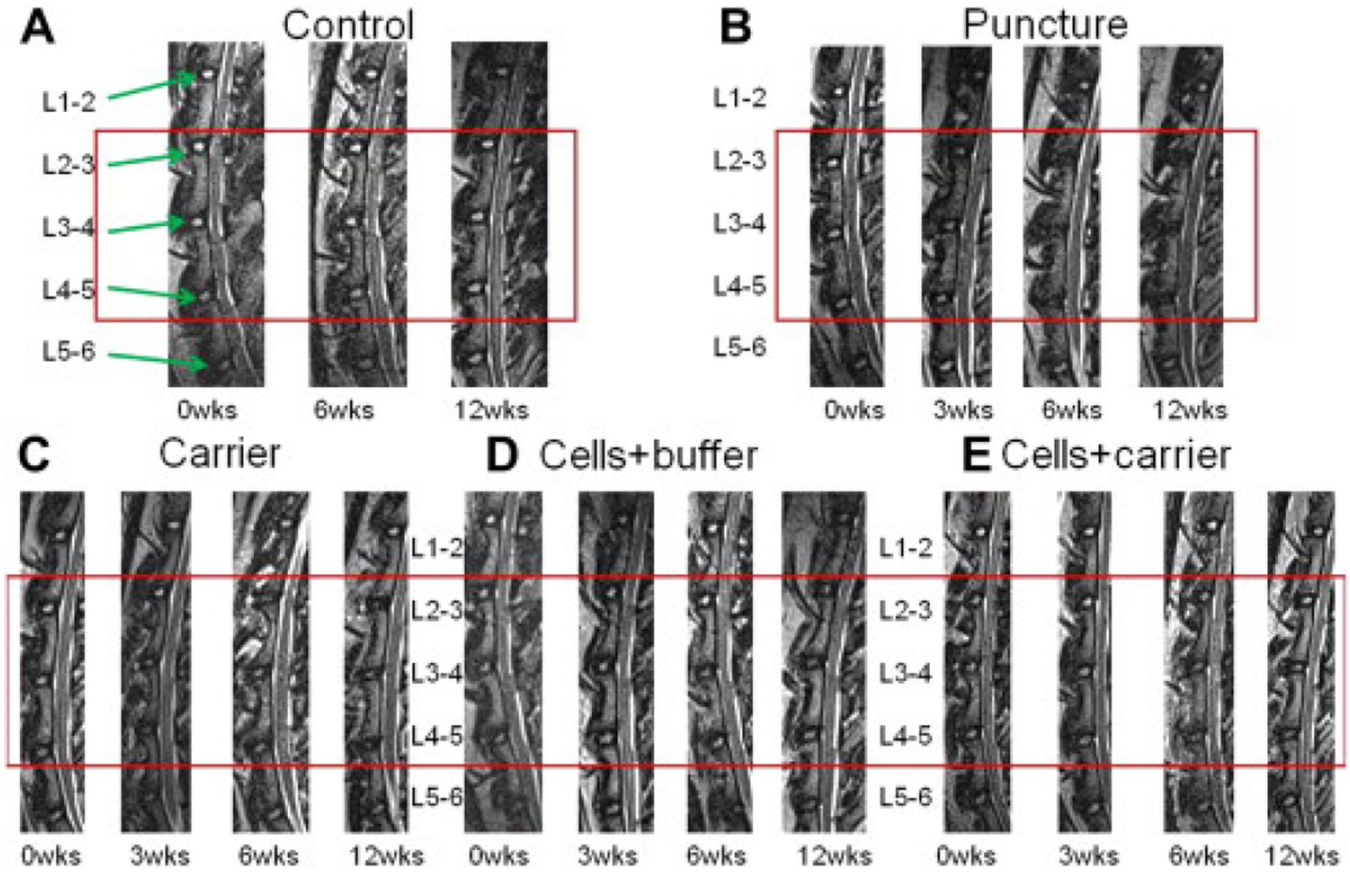

Figure 1.

Lumbar spine magnetic resonance images (MRIs). Sample T2-weighted midsagittal lumbar MRI images of L1–L2 through L5–L6 at time-points 0, 3, 6, and 12 weeks. Rabbits have six lumbar vertebrae. The punctured discs (L2–L3, L3–L4, and L4–L5) are outlined by the red boxes. The adjacent unpunctured discs for each rabbit (L1–L2 and L5–L6) do not show any qualitative evidence of degeneration. The discs of the (A) control group did not degenerate, as expected. (B) The punctured discs became smaller and darker across time-points, suggesting degeneration. (C) The discs that were punctured and then treated with carrier, (D) human umbilical tissue–derived cells (hUTC)+buffer, and (E) hUTC+carrier demonstrate less evidence of degeneration across time-points compared with the (B) punctured discs. Each group consisted of six rabbits (18 discs).

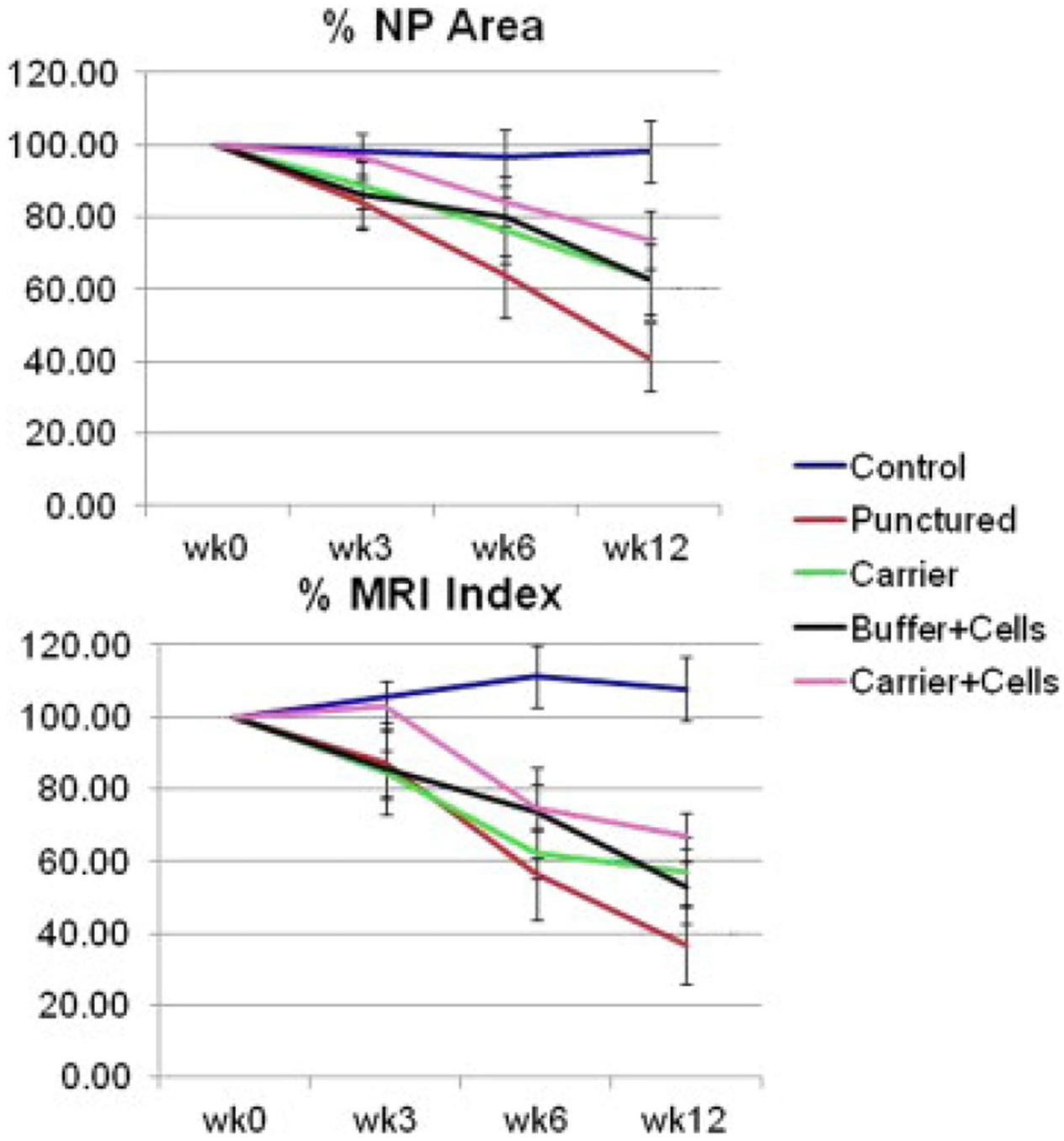

Figure 2.

Quantitative MRI analysis. Average data for (Top) NP area and (Bottom) MRI Index combining L2–L3, L3–L4, and L4–L5 (the treated discs) for each rabbit group, expressed as a percent of the Time 0 value, demonstrates that the punctured group undergoes the largest decrease in area and MRI Index across time-points. The groups that were punctured and subsequently treated with carrier or cells+buffer undergo lesser decrease in area and Index, whereas the group treated with cells+carrier undergoes the least decrease in area and Index. Error bars represent standard error. Each group consisted of six rabbits (18 discs).

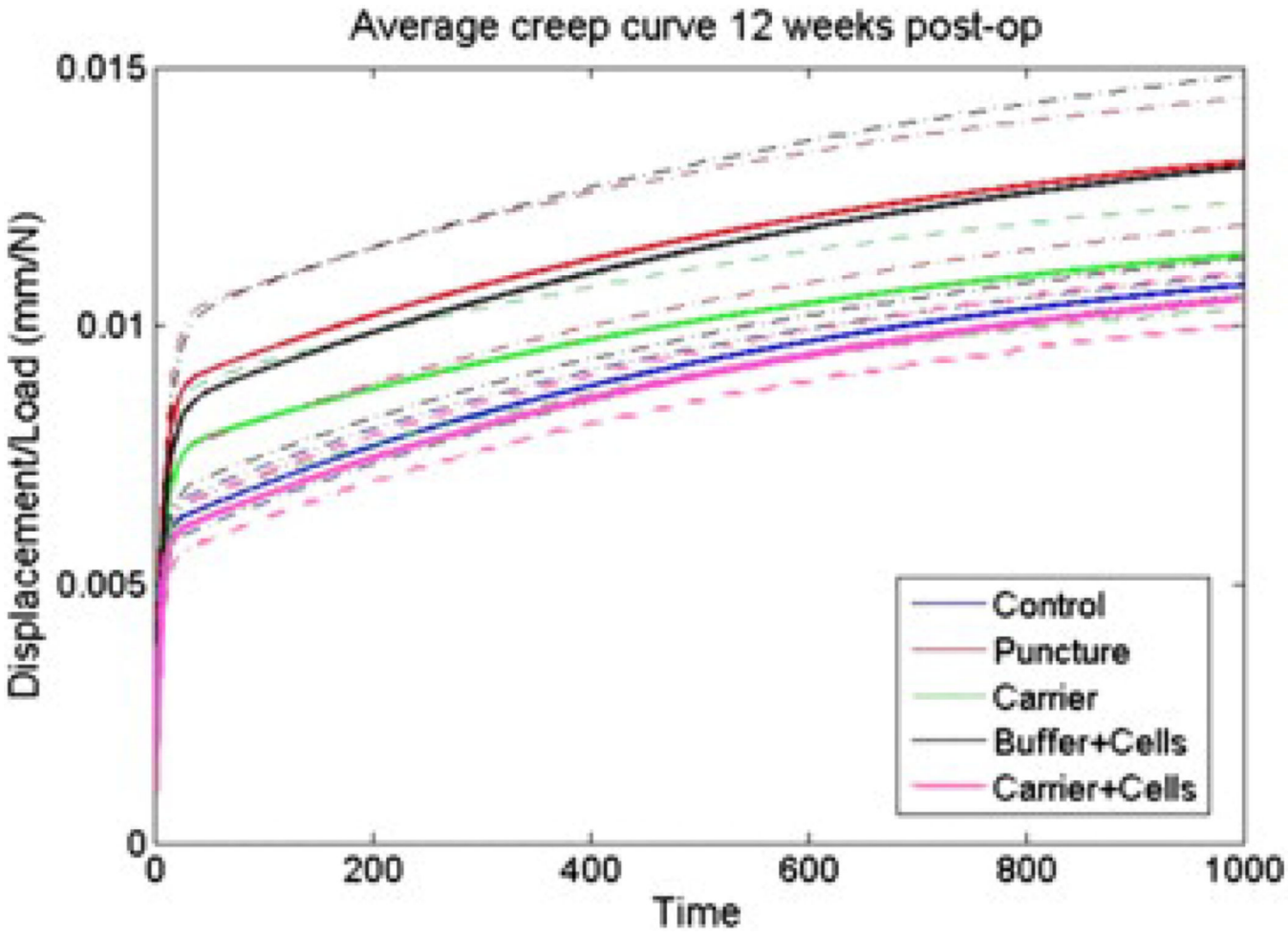

Figure 3.

Creep curves. Average normalized total displacement (ramp phase+creep) curves of potted L3–L4 functional spinal units after 12 weeks were generated for each condition. Axial testing generates distinct appearing creep curves in the early phase of testing (time, 0–200 seconds). Dotted boundaries represent standard error of measurement. The curves generated for puncture and buffer+cells appear similar, as do curves for control and carrier+cells. Each of these groups appears distinct from the curve generated for the carrier group. Each group consisted of six rabbits (six discs). Post-op, postoperative.

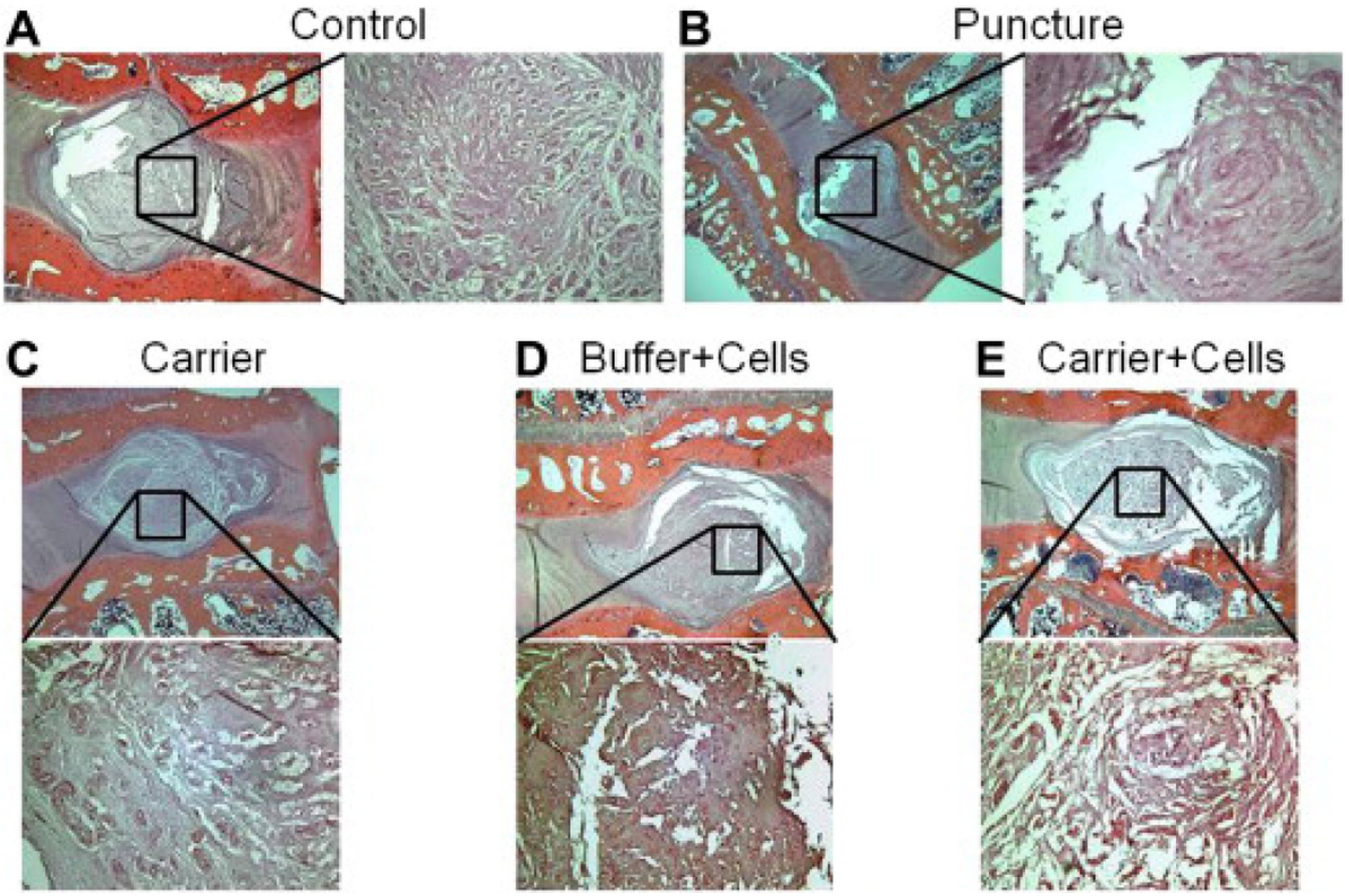

Figure 4.

Histology. Sagittal slices of disc L4–L5 obtained after sacrifice at 12 weeks for each treatment group ([A] Control, [B] Puncture, [C] Carrier, [D] Buffer + Cells, [E] Carrier + Cells), stained with hematoxylin and eosin, and magnified ×20 and ×100. Treatment helps restore some aspects of cellularity and architecture. Each group consisted of six rabbits (six discs).

Table

Overview

Time	Control (N=6 rabbits)	Puncture (N=6 rabbits)	Cell (N=6 rabbits)	Carrier (N=6 rabbits)	Cell+carrier (N=6 rabbits)
0 wks	MRI	MRI Puncture surgery L23, L34, L45	MRI Puncture surgery L23, L34, L45	MRI Puncture surgery L23, L34, L45	MRI Puncture surgery L23, L34, L45
3 wks	MRI	MRI	MRI Injection surgery L23, L34, L45 10^5 cells/15 μL PBS/disc	MRI Injection surgery L23, L34, L45 15 μL hydrogel/disc	MRI Injection surgery L23, L34, L45 10^5 cells/15 μL hydrogel/disc
6 wks	MRI	MRI	MRI	MRI	MRI
12 wks	MRI Sacrifice Histo L4–L5 BioM L3–L4	MRI Sacrifice Histo L4–L5 BioM L3–L4	MRI Sacrifice Histo L4–L5 BioM L3–L4	MRI Sacrifice Histo L4–L5 BioM L3–L4	MRI Sacrifice Histo L4–L5 BioM L3–L4

MRI, magnetic resonance imaging; PBS, phosphate-buffered saline; Histo, histology; BioM, biomechanics.